Aerosol and Air Quality Research, 15: 1469–1484, 2015

ISSN: 1680-8584 print / 2071-1409 online
doi: 10.4209/aaqr.2014.10.0256

Decomposition of Organic Chemicals in the Air and Inactivation of Aerosol-Associated Influenza Infectivity by Photocatalysis

Tohru Daikoku[1], Masaya Takemoto[1], Yoshihiro Yoshida[1], Tomoko Okuda[1], Yasuaki Takahashi[2], Kanji Ota[2], Fumio Tokuoka[3], Akira T. Kawaguchi[4], Kimiyasu Shiraki[1*]

[1] *Department of Virology, University of Toyama, 2360 Sugitani, Toyama 930-0194, Japan*
[2] *OTA Incorporated, 5-10-7 Minamisuna, Koto-ku, Tokyo 136-0076, Japan*
[3] *Shonan Ceramics Corporation, 32-3 Horikawa, Hadano, Kanagawa 259-1305, Japan*
[4] *Department of Cell Transplantation and Regenerative Medicine, Tokai University School of Medicine, 143 Shimokasuya, Isehara, Kanagawa 259-1193, Japan*

ABSTRACT

Efficiency of photocatalysis depends on the surface area and materials, and we have prepared a porous ceramic substrate coated with nanosized-TiO_2 for a photocatalytic air cleaner. The surface of the porous ceramic was coated with nano-sized TiO_2 and total surface area of the board (30 × 30 × 1 cm) was 7,432 m^2, being 14,864 m^2 as the total area in the cleaner consisting of two boards and intervened black lamps. Eighty percent of 5 ppm acetaldehyde was decomposed and generated 8 ppm of carbon dioxide for 3 hours efficiently and continuously by passing through the TiO_2-coated ceramic (5 × 10 × 1 cm) under black light. Particulate dioxins (40 pg/m^3) and gaseous dioxins (16 pg/m^3) were removed by 7.5 and 2.8 pg/m^3 by passing through four TiO_2-coated ceramic (30 × 30 × 2 cm) under black-light, indicating about 80% of dioxin was decomposed by the photocatalysis. This photocatalysis system was applied for inactivation of influenza aerosol. Influenza infection is spread efficiently by inhalation of aerosol-associated influenza virus. The aerosol-associated infectivity produced by nebulizer in a 754 liter cubic space was more than 10,000 plaque-forming units and was detectable for up to 30 minutes. The aerosol-associated infectivity of influenza virus was eliminated within five minutes by a photocatalytic air cleaner. The infectious aerosol-associated influenza would accumulate by the continuous production by cough and sneeze in the closed space, resulting in the efficient influenza infection. Thus a photocatalytic air cleaner efficiently decomposed organic chemicals including acetaldehyde and dioxins and inactivated aerosol-associated influenza virus infectivity.

Keywords: Dioxins; Acetaldehyde; Airborne infection; Nanosized-TiO_2.

INTRODUCTION

Organic chemicals are decomposed by reactive oxygen species generated photocatalysis with titanium dioxide (TiO_2) and light (Fujishima and Honda, 1972). We have developed the efficient system for maximize the photocatalysis by coating nanosized-TiO_2 to a porous ceramic substrate to increase the surface area and applied it for decomposing organic chemicals in the vapor phase and inactivating aerosol-associated influenza infectivity. Photocatalysis by TiO_2 produces negative electrons (e^-: electron hole) and positive holes (h^+) and generates superoxide anions ($O_2 + e^- \rightarrow O_2^-$) and hydroxyl radicals ($OH^- + h^+ \rightarrow \cdot OH$). TiO_2 on the surface of ceramic is exposed to ultraviolet light with a shorter wavelength than 400 nm and e^- and h^+ are generated around the surface of the ceramic. The generated e^- reacts with O_2 (oxygen) in the air and generates O_2^- (superoxide anion). The h^+ reacts H_2O and generates OH (hydroxyl radical). These O_2^- and OH radicals react and decompose organic chemicals and inactivate microbes. Titanium is non-corrosive and environmentally safe; it is used as a food additive and in cosmetics, especially sun blockers. We have developed the efficient photocatalytic system using porous ceramic coated with photocatalytic nano-TiO_2. The power of photocatalysis on the TiO_2-coated surface depends on the strength of the light and the cleanness of the surface. The TiO_2-coated ceramic is stable and reusable by cleaning the surface with deionized water, when the surface is contaminated and attached with sulfuric or nitric compounds decomposed from the organic compounds. Decomposition of acetaldehyde and dioxins and inactivation of influenza virus infectivity are shown using our photocatalytic porous ceramic system in this study.

* Corresponding author.
Tel.: 81-76-434-7255; Fax: 81-76-434-5020
E-mail address: kshiraki@med.u-toyama.ac.jp

Photocatalysis decomposes acetaldehyde (Asahi *et al.*, 2001; Huang *et al.*, 2009; Li *et al.*, 2012) and dixions (Lu *et al.*, 2011; Vallejo *et al.*, 2014). Inactivation of bacteria and viruses on a surface in the liquid by photocatalysis has been reported to be effective (Rizzo, 2009; Guglielmotti *et al.*, 2011; Zan *et al.*, 2007). We observed the efficient inactivation of aerosol-associated infectivity of influenza virus by the photocatalytic air cleaner with a titanium-coated surface that emitted the superoxide anions and hydroxyl radicals due to exposure to light in this study.

Influenza is prevented by influenza vaccine and treated with neuraminidase inhibitors. We have characterized a novel anti-influenza drug, T-705 (favipiravir), and it will be added as a new type of anti-influenza drug (Furuta *et al.*, 2002; Takahashi *et al.*, 2003; Furuta *et al.*, 2005, 2009). Thus influenza infection can be controlled by vaccination and treatment with anti-influenza drugs. However the infectivity of the aerosol-associated influenza has not been characterized.

Experimental and clinical evidence suggests that influenza infection by a small-particle aerosol (particle diameter < 10 μm) is more efficient than that by larger droplets or contact infection (Andrewes, 1941; Knight, 1980; McLean, 1961; Moser *et al.*, 1979; Schulman and Kilbourne, 1962; Goldmann, 2000). Transmission of influenza occurs mostly via aerosols generated by coughs and sneezes. The 72% of 54 passengers aboard an airplane were infected with influenza when the ventilation system was inoperative during a three-hour delay, and the closed space with inefficient ventilation accounted for the high infection rate (Moser *et al.*, 1979).

The size distribution of coughed droplets is multimodal. The average size of the droplet nuclei produced by a cough is 0.58–5.42 μm, and 82% of droplet nuclei are 0.74–2.12 μm. The total average size distribution of the coughed droplets is 0.62–15.9 μm, and the average mode size is 8.35 μm. Coughed droplets show three peaks at approximately 1 μm, 2 μm, and 8 μm (Yang *et al.*, 2007). Considerable variability among cougher or sneezer is observed, and the average size of droplets captured on glass slides and viewed through a microscope is about 50–100 μm (Xie *et al.*, 2009). The exhaled pulmonary bioaerosol of a sneeze (particle diameter < 10 μm) is estimated to be 10^2 times than that of a cough (Chen *et al.*, 2009). The sizes of the largest droplets that totally evaporate before landing 2 m away are between 60 and 100 μm for respiratory exhalation flows (Xie *et al.*, 2007). Exhaled breath generates 3.2 to 20 influenza virus RNA copies per minute, although their infectivity was not evaluated. Influenza virus may be contained in fine particles generated during tidal breathing, suggesting that fine particle aerosols may play a role in influenza transmission. Over 87% of particles exhaled were under 1 μm in diameter (Fabian *et al.*, 2008).

Particles of the size of 1–3 μm are preferentially deposited in the lower airways of the lung (Knight, 1980; Heyder, 1986; Isaacs and Martonen, 2005). Infection of volunteers can best be achieved by aerosol-associated virus. The human infectious dose 50 of wild-type influenza A virus administered intranasally by drops is 127 to 320 of the median tissue culture infective dose ($TCID_{50}$), and that of virus delivered by an aerosol is 0.6 to 3 $TCID_{50}$ (Alford *et al.*, 1966; Couch *et al.*, 1971; Murphy *et al.*, 1973; Couch and Kasel, 1983).

There is no convenient and conventional system for disinfecting the aerosol-associated infectivity of influenza virus except for its removal by air filtration through HEPA filters. Here we applied photocatalysis, which is known to decompose pollutants and malodorous chemicals, for inactivation of aerosol-associated infectivity. Thus, the system may be suitable for decomposing organic chemicals including acetaldehyde and dioxins and disinfecting aerosol-associated influenza viruses in a closed space with low ventilation or a public space during an influenza epidemic.

METHOD

Photocatalytic Air Cleaner

Fig. 1 shows the schematic view of the structure of the air cleaner and the porous ceramic substrate. Porous ceramic (Bridgestone ceramic foam) was purchased from Narita Seitosho KK, Seto City, Japan. The photocatalyitic TiO_2 was purchased from the Ishihara Sangyo Kaisha, LTD. Osaka, Japan. The coating of TiO_2 on the surface of porous ceramic was performed by fixing the fine TiO_2 nanoparticles on the wet surface of the porous ceramic under negative pressure conditions in order to coat them on the inside surface of concaved pores. The surface of the porous ceramic was coated with the nano-sized TiO_2 and the specific surface area of solids was determined by gas adsorption using the Brunauer-Emmett-Teller (BET) method. Total surface area of the board (30 × 30 × 1 cm) was 7,432 m^2, being 14,864 m^2 as the total area in the cleaner consisting of two boards and intervened black lamps.

Performance Evaluation of Photocatalysis to Acetaldehyde and Dioxins

Decomposition of acetaldehyde was analyzed by passing through the nano-sized TiO_2-coated porous ceramic with 5 × 10 cm size and 1cm thick (approximately 408.8 m^2 as total surface area) under 1 mW black light (wavelength 365 nm) per 1 cm^2. The test was performed according to the procedure of JIS R1701-2 defined by the Japanese Industrial Standards Committee. Acetaldehyde at 5 ppm and 1.56% water was passed at the rate of 1 L/min at 25 ± 2°C and detection of acetaldehyde and carbon dioxide was performed by Flame Ionization Detector (GC-2014AFF, Shimadz, Kyoto, Japan) at the Kanagawa Academy of Science and Technology.

Decomposition of dioxins were examined by passing through four nano-sized TiO_2-coated porous ceramic boards (30 × 30 cm size and 2 cm thick) and three sets of black lamps in three intervened spaces under 1 mW black light (wavelength 365 nm) per 1 cm^2 at the flow speed of 1 m/sec. Particulate and gaseous dioxins were collected on the dust collection filter paper and polyurethane foam, respectively, collected by the high volume sampler. Dioxins produced in the waste incineration plant were used for decomposition of particulate and gaseous dioxins. The concentrations of particulate and gaseous dioxins at the inlet and outlet were determined and the difference in the amount of dioxins between them was calculated as the amount of decomposed dioxins. Particulate and gaseous dioxins were analyzed at the

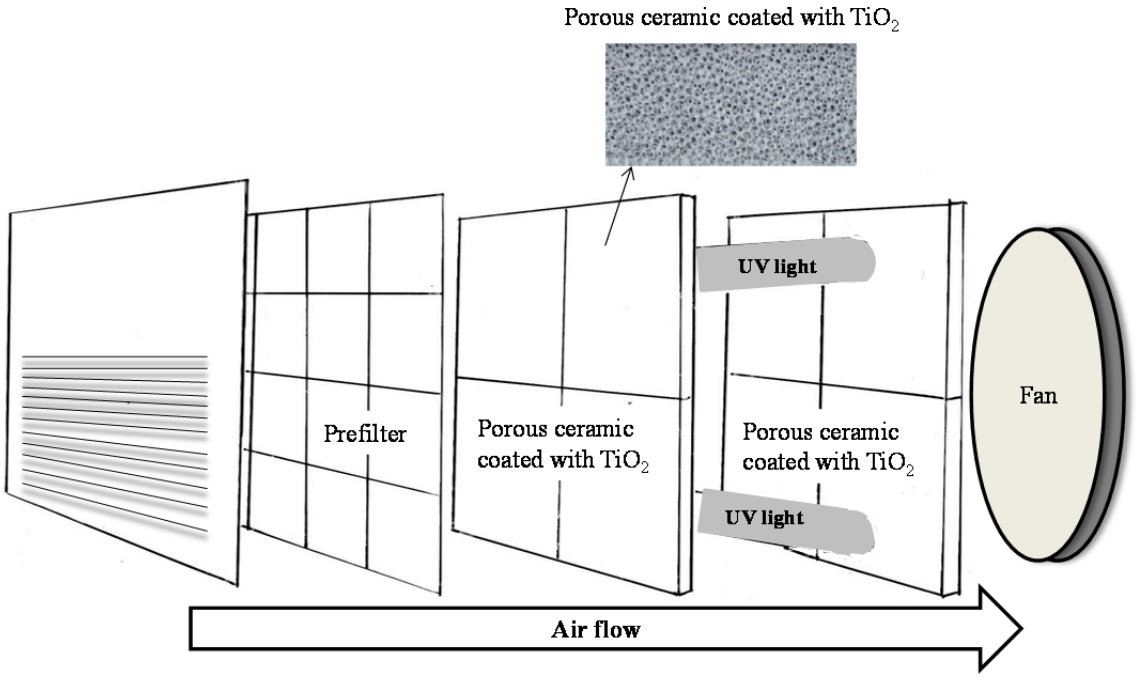

Fig. 1. The schematic view of the structure of the air cleaner and the porous ceramic substrate. The surface of the porous ceramic was coated with nano-sized TiO_2 and total surface area of the board was 7,432 m^2, being 14,864 m^2 as the total area in the cleaner. The flow rate of the air conditioner is 0.1 m/s, 0.2 m/s, and 0.4 m/s of 3 stages.

inlet and outlet according to the dioxin exposure prevention guidelines in waste incineration facilities in work from the Ministry of Health, Labour and Welfare, Japan, by gas-chromatograph coupled with mass spectrometer at the Eurofins Nihon Kankyo K.K.

Aerosol-Associated Infectivity of Influenza Virus

Influenza virus A/PR/8/34 (H1N1) was propagated in Madin-Darby canine kidney (MDCK) cells, and virus stocks were prepared from infected-cultured cells as reported previously (Kurokawa *et al.*, 1996a, b; Furuta *et al.*, 2002; Kurokawa *et al.*, 2002, 2010). The cells were grown and maintained in minimum essential medium (MEM) supplemented with 8% and 2% fetal bovine serum, respectively. Duplicate cultures of MDCK cells in 60-mm plastic dishes were infected with 100 plaque-forming units (PFU)/0.2 mL of influenza virus for 1 h at room temperature. Cells were overlaid with 5 ml nutrient agarose (0.8%) medium and cultured at 37°C for 2–3 days. The infected cells were fixed with 5% formalin and stained with 0.03% methylene blue solution. The number of plaques was counted under a dissecting microscope (Kurokawa *et al.*, 1996a).

Inactivation of Aerosol-Associated Infectivity of Influenza Virus

Fig. 2 shows the system for assaying the aerosol-associated infectivity of influenza virus in the closed space. The photocatalytic air cleaner used was a virus-shelter SC125-TB (O.T.A Inc., Tokyo, Japan). The air was filtered through a lighted ceramic filter coated with titanium dioxide under an electric fan in the photocatalytic air cleaner.

A nebulizer (JP-HS) purchased from J.P. Clarus Co., Ltd. was used to produce and distribute particles 7–15 μm in diameter. Ten milliliters of influenza virus solution containing 4.0×10^8 PFU was nebulized into the 91 × 91 × 91-cm space (754 liters). A 40-L volume of the air containing aerosol-associated influenza virus was serially transferred from air bag A through the cubic space to air bag B (Fig. 2). The trapped air was filtered through a 0.45 μm cellulose-acetate membrane filter (47 mm in diameter, Millipore Co., Billerica, MA) by an aspirator vacuum pump. The experiments were performed once in a day at 22°C with 50–60% humidity to perform each experiment in the similar condition. The filter was cut into the pieces, immersed and then vigorously rinsed in MEM. The medium was centrifuged, and its supernatant was serially diluted and inoculated into the cells in 6-cm Petri dishes for the plaque assay to evaluate the infectivity trapped on the filter. Influenza virus RNA trapped on the a 0.45 μm cellulose-acetate membrane filter was used for virus infectivity for plaque assay and RNA in the 50 μL of resultant supernatants was extracted using a High Pure Viral RNA kit (Roche Diagnostics, Mannheim, Germany) according to the manufacturer's protocol. Reverse transcription (RT) was carried out by Reva-Tra Ace kit (Toyobo Bio, Osaka, Japan) using an influenza viral RNA specific primer Uni12 (5'-agcgaaagcagg-3') in a 10 μL reaction mixture at 37°C for 1 h. Two microliters of the RT reaction mixture was then used for real-time PCR by using an influenza M gene–specific primer set, forward primer (5'-CGCTCAGACATGAGAACAGAATGG-3') and reverse primer (5'-TAACTAGCCTGACTAGCAACCTC-3'), SYBR green PCR Master Mix (Kapa Biosystems, Cape Town, South Africa). Before the quantitative PCR, the mixture was

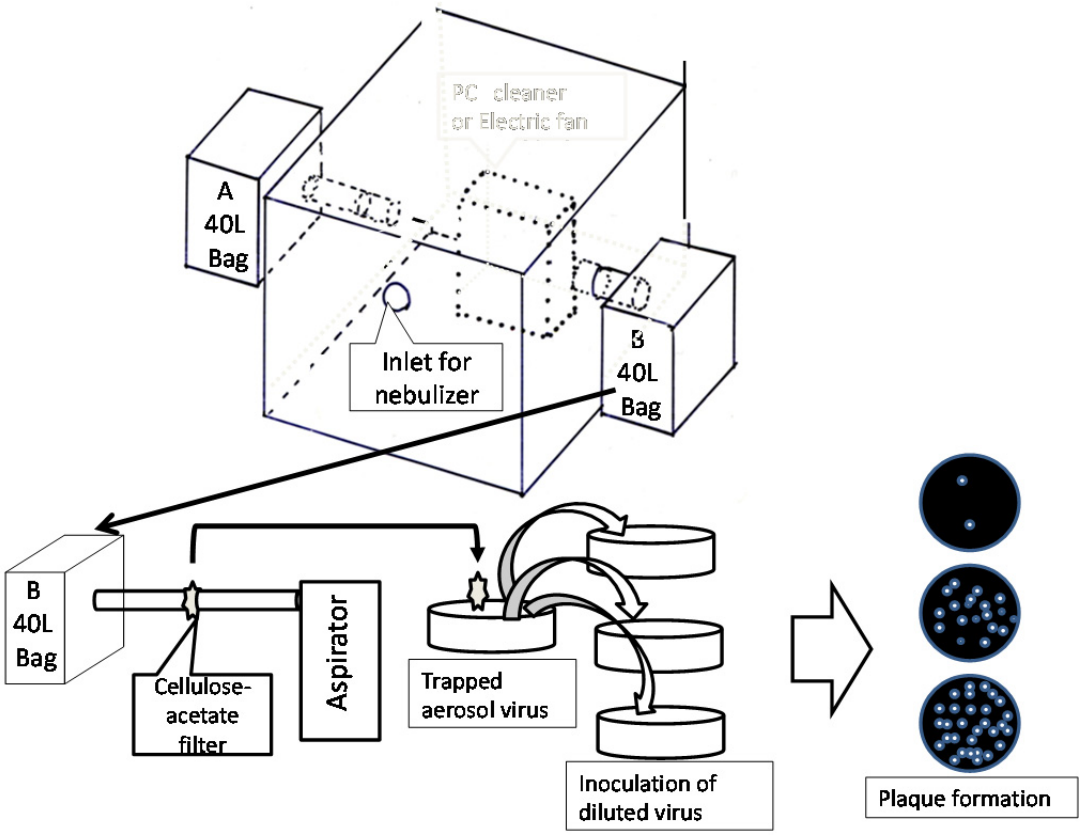

Fig. 2. Diagram of the system to assay aerosol-associated infectivity of influenza virus. Aerosol-associated influenza virus was injected by a nebulizer into a 91 × 91 × 91-cm cubic space (754 Liters (L)), and a 40-L volume of air was slowly blown from bag A to bag B. Forty L in air bag A was supplied to the cubic space of 754 L by closing the A, and at the same time the 40 L of the air was fed to bag B by opening bag B at the indicated times. The air in the bag was filtered through a 47-mm diameter 0.45-μm pore cellulose-acetate filter, and the filter was cut into pieces and immersed in the medium. Then the trapped infectious virus was suspended in the medium, diluted, and inoculated into MDCK cells for determination of the plaque number. The assay was performed in the presence of an electric fan with or without a photocatalytic (PC) air cleaner.

incubated at 95°C for 10 min. The quantitative PCR reaction was performed at 95°C for 10 sec, 57°C for 20 sec, and 72°C for 30 sec for 45 cycles, and the levels of PCR products were monitored with a Takara Dice thermal cycler for real-time PCR system and analyzed with Takara Real-time PCR software (Takara Bio Inc., Otsu, Shiga, Japan).

RESULTS

Decomposition of Acetaldehyde and Dioxins by Photocatalysis

Fig. 3 shows the decomposition profile of acetaldehyde to carbon dioxide. When a gas containing 5 ppm acetaldehyde and 1.56% water was passed through the photocatalytic air cleaner at a rate of 1 L/min at 25 ± 2°C and humidity of 40 ± 10%, 78.36% of the acetaldehyde was stably removed in a single passage for 180 min (Japan Industrial Standards Committee). Decomposition of acetaldehyde to carbon dioxide and water by photo catalysis is as follows; $CH_3CHO + 6OH + O_2 \rightarrow 2CO_2 + 5H_2O$. Thus the molar ratios of input acetaldehyde and output carbon dioxide is one acetaldehyde molecule and 2 carbon dioxide molecules. Eighty percentages of acetaldehyde of 5 ppm was 4 ppm and 4 ppm of aldehyde was decomposed to 8 ppm of carbon dioxide as shown in Fig. 3. The ratio of acetaldehyde and carbon dioxide with increased humidity was consistent as the decomposition of acetaldehyde to carbon dioxide and water with their molar ratios.

Particulate and gaseous dioxins at the inlet and outlet of the air through the photocatalytic air cleaner system were examined at the flow speed of 1m/sec according to the gas-chromatograph coupled with mass spectrometer and the results of two experiments were shown in Table 1 and 2.

Particulate dioxins of 47 pg/m^3 (Table 1A) at the inlet were removed to 8.7 pg/m^3 (Table 1B) at the outlet and the removal of particulate dioxins was 81.49% by the single pass in the experiment 1. Particulate dioxins of 40 pg/m^3 (Table 1C) at the inlet were removed to 7.5 pg/m^3 (Table 1D) at the outlet and the removal of particulate dioxins was 81.25% by the single pass in the experiment 2.

Gaseous dioxins of 35 pg/m^3 (Table 2A) at the inlet were removed to 3.0 pg/m^3 (Table 2B) at the outlet and the removal of gaseous dioxins was 91.43% by the single pass in the experiment 1. Gaseous dioxins of 16 pg/m^3 (Table 2C) at the inlet were removed to 2.8 pg/m^3 (Table 2D) at the outlet and the removal of gaseous dioxins was 82.5% by

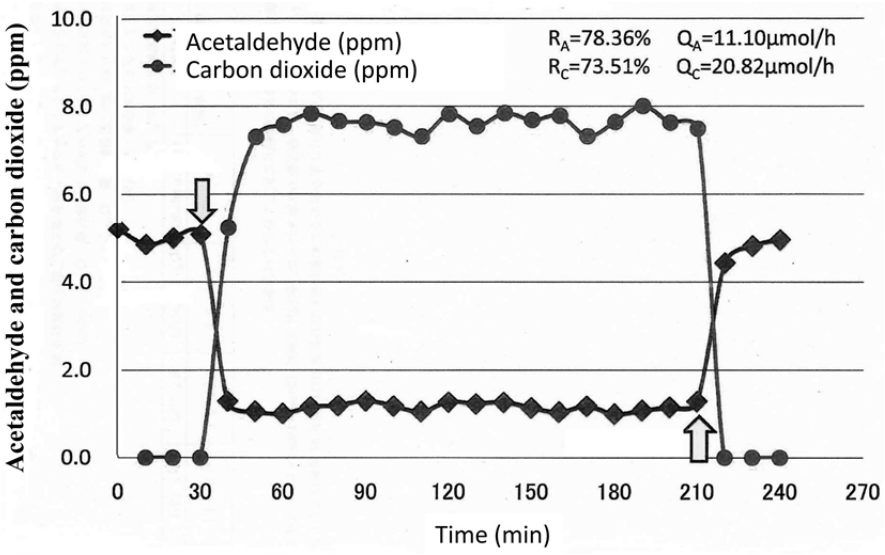

Fig. 3. The decomposition profile of acetaldehyde to carbon dioxide and water using the porous ceramic coated with nano-sized TiO_2 with the size of 5 × 10 cm with 1cm wide (approximately 185.8 m^2) irradiated with black light. When the black light was on at 30 min, acetaldehyde decreased and carbon dioxide increased. When black light was off at 210 min, acetaldehyde concentration increased and carbon dioxide decreased to the level without black light. The figure is modified from the original figure (Takahashi, 2011). RA, Acetaldehyde removal rate. RC, Carbon dioxide conversion rate. QA, Removal amount of acetaldehyde per hour. QC, Carbon dioxide conversion amount per hour.

the single pass in the experiment 2. Particulate and gaseous dioxins were removed by 81.49 and 81.25%, and 91.43 and 82.5%, respectively, in two independent experiments. All of the chemicals in particulate and gaseous dioxins were universally and efficiently decomposed and the decomposition specificity to the chemicals was not noted as shown in Table 1 and 2.

We excluded the possibility of capturing dioxins on the surface of ceramic. The amount of dioxins captured on the ceramic was assayed and was 0.88 pg, when total removal amount was 317.33 pg from the reduction between the inlet and outlet. Therefore the decomposed and captured dioxins were 99.72 and 0.28%, respectively. This indicated that at least 80% of dioxins were decomposed by the photocatalysis with a nano-sized TiO_2-coated porous ceramic under black light.

Inactivation of Aerosol-Associated Infectivity of Influenza Virus by Photocatalysis

One-hundred microliters of virus solution containing 4.0 × 10^6 PFU was applied to the cellulose-acetate membrane filter, and a total of 4.0 × 10^5 PFU of infectious virus was recovered in the rinsing solution. Thus, although the virus numbers in the aerosol and solution were different, the recovery of infectious virus from the cellulose-acetate membrane filter was 10%.

The aerosol-associated infectivity ranged from 10,550 to 49,924 PFU in the 754 L space at time 0 and the infectivity in the cubic space decreased with time for 30 min under an electric fan without black light (Fig. 4(a)). Decay of infectivity was determined under PC cleaner with and without a black light. The aerosol-associated infectivity was quickly inactivated and was undetectable within 5 min by photocatalysis with TiO_2 irradiated by black light (Fig. 4(b)), while 2,072 and 7,159 PFU were detected at 5 min under an electric fan without black light (Fig. 4(a)). Influenza virus RNA was quantitated by RT-PCR but the plaque assay was more sensitive than the RNA copy assay (data not shown).

DISCUSSION

The device for a photocatalytic air cleaner was evaluated by decomposition of aldehyde and dioxins, and inactivation of aerosol-associated influenza virus infectivity. Acetaldehyde was efficiently decomposed by passing once through a nano-sized TiO_2-coated porous ceramic. The cleaner is consisting of two ceramic boards intervened by black-light and the efficiency of decomposition might be better than a single pass as shown in Fig. 1. Particulate and gaseous dioxins were examined according to the gas-chromatograph coupled with mass spectrometer by the Eurofins Nihon Kankyo K.K. Particulate dioxins (40 pg/m^3) and gaseous dioxins (16 pg/m^3) were removed by 7.5 and 2.8 pg/m^3, indicating more than 80% of dioxin was decomposed by the photocatalysis with a nano-sized TiO_2-coated porous ceramic. Thus the photocatalytic air cleaner showed efficient decomposition of organic chemicals and the efficiency of this device was examined for the inactivation of aerosol-associated influenza infectivity.

The photocatalytic ceramic is physically and chemically stable and can be used until broken. Sulfur compounds and nitrogen compounds are decomposed to sulfuric acid and nitric acid and these compounds binds and accumulates on the surface, resulting in the inhibition of photocatalyis. These can be removed by washing with deinonized water and then the photocatalytic activity recovers.

Table 1A. Particulate dioxins before photocatalysis (Experiment 1).

	Dioxins	measured concentration (pg/m^3)	quantification limit of sample (pg/m^3)	detection limit of sample (pg/m^3)	toxic equivalency factor (TEF)	toxic equivalent (TEQ) ($pg\text{-}TEQ/m^3$)
PCDDs	1,3,6,8-TeCDD	0.21	0.05	0.02	-	
	1,3,7,9-TeCDD	0.10	0.05	0.02	-	
	2,3,7,8-TeCDD	0.05	0.05	0.02	1	0.05
	TeCDDs	0.62	-	-	-	
	1,2,3,7,8-PeCDD	0.07	0.06	0.02	1	0.07
	PeCDDs	1.2	-	-	-	
	1,2,3,4,7,8-HxCDD	(0.05)	0.11	0.04	0.1	0.005
	1,2,3,6,7,8-HxCDD	0.21	0.11	0.04	0.1	0.021
	1,2,3,7,8,9-HxCDD	0.12	0.11	0.04	0.1	0.012
	HxCDDs	2.4	-	-	-	
	1,2,3,4,6,7,8-HpCDD	2.6	0.11	0.04	0.01	0.026
	HpCDDs	5.3	-	-	-	
	OCDD	13	0.13	0.04	0.0003	0.0039
	Total PCDDs	23	-	-	-	0.19
PCDFs	1,2,7,8-TeCDF	0.07	0.06	0.02	-	
	2,3,7,8-TeCDF	(0.05)	0.06	0.02	0.1	0.005
	TeCDFs	2.9	-	-	-	
	1,2,3,7,8-PeCDF	0.32	0.06	0.02	0.03	0.0096
	2,3,4,7,8-PeCDF	0.32	0.06	0.02	0.3	0.096
	PeCDFs	5.2	-	-	-	
	1,2,3,4,7,8-HxCDF	0.43	0.11	0.04	0.1	0.043
	1,2,3,6,7,8-HxCDF	0.46	0.11	0.04	0.1	0.046
	1,2,3,7,8,9-HxCDF	(0.06)	0.11	0.04	0.1	0.006
	2,3,4,6,7,8-HxCDF	0.77	0.11	0.04	0.1	0.077
	HxCDFs	5.2	-	-	-	
	1,2,3,4,6,7,8-HpCDF	2.3	0.11	0.04	0.01	0.023
	1,2,3,4,7,8,9-HpCDF	0.40	0.11	0.04	0.01	0.0040
	HpCDFs	4.1	-	-	-	
	OCDF	1.9	0.15	0.05	0.0003	0.00057
	Total PCDFs	19	-	-	-	0.31
Total (PCDDs + PCDFs)		42	-	-	-	0.50
coplanar-PCBs	3,4,4',5-TeCB	(0.08)	0.11	0.04	0.0003	0.000024
	3,3',4,4'-TeCB	0.27	0.11	0.04	0.0001	0.000027
	3,3',4,4',5-PeCB	0.47	0.11	0.04	0.1	0.047
	3,3',4,4',5,5'-HxCB	0.29	0.11	0.04	0.03	0.0087
	Non-ortho PCBs	1.1	-	-	-	0.056
	2',3,4,4',5-PeCB	(0.05)	0.11	0.04	0.00003	0.0000015
	2,3',4,4',5-PeCB	1.8	0.11	0.04	0.00003	0.000054
	2,3,3',4,4'-PeCB	0.80	0.11	0.04	0.00003	0.000024
	2,3,4,4',5-PeCB	(0.10)	0.11	0.04	0.00003	0.0000030
	2,3',4,4',5,5'-HxCB	0.26	0.11	0.04	0.00003	0.0000078
	2,3,3',4,4',5-HxCB	0.68	0.11	0.04	0.00003	0.0000204
	2,3,3',4,4',5'-HxCB	0.30	0.11	0.04	0.00003	0.0000090
	2,3,3',4,4',5,5'-HpCB	0.48	0.11	0.04	0.00003	0.0000144
	Mono-ortho PCBs	4.5	-	-	-	0.00013
Total coplanar-PCBs		5.6	-	-	-	0.056
Total (PCDDs + PCDF + coplanar-PCBs)		47	-	-	-	0.55

1. The values of 1,2,3,7,8-PeCDF and 1,2,3,4,7,8-HxCDF include those of 1,2,3,4,8-PeCDF and 1,2,3,4,7,9-HxCDF, respectively, because of inability to resolve them on chromatogram.
2. "()" in "measured concentration" column means the value between quantification limit and detection limit.
3. "N.D." in "measured concentration" column means "not detected".
4. The value of TEF is based on WHO-TEF (2006).
5. TEQ was calculated by using either the value of "measured concentration" when they could be detected or the half value of "detection limit" when they could not detected.

Table 1B. Particulate dioxins removed after photocatalysis (Experiment 1).

	Dioxins	measured concentration (pg/m^3)	quantification limit of sample (pg/m^3)	detection limit of sample (pg/m^3)	toxic equivalency factor (TEF)	toxic equivalent (TEQ) ($pg\text{-}TEQ/m^3$)
PCDDs	1,3,6,8-TeCDD	(0.03)	0.05	0.02	-	
	1,3,7,9-TeCDD	N.D.	0.05	0.02	-	
	2,3,7,8-TeCDD	N.D.	0.05	0.02	1	0.01
	TeCDDs	0.03	-	-	-	
	1,2,3,7,8-PeCDD	(0.03)	0.06	0.02	1	0.03
	PeCDDs	0.21	-	-	-	
	1,2,3,4,7,8-HxCDD	N.D.	0.11	0.04	0.1	0.002
	1,2,3,6,7,8-HxCDD	N.D.	0.11	0.04	0.1	0.002
	1,2,3,7,8,9-HxCDD	N.D.	0.11	0.04	0.1	0.002
	HxCDDs	0.39	-	-	-	
	1,2,3,4,6,7,8-HpCDD	0.67	0.11	0.04	0.01	0.0067
	HpCDDs	1.4	-	-	-	
	OCDD	3.3	0.13	0.04	0.0003	0.00099
	Total PCDDs	5.3	-	-	-	0.054
PCDFs	1,2,7,8-TeCDF	N.D.	0.06	0.02	-	
	2,3,7,8-TeCDF	N.D.	0.06	0.02	0.1	0.001
	TeCDFs	0.18	-	-	-	
	1,2,3,7,8-PeCDF	(0.03)	0.06	0.02	0.03	0.0009
	2,3,4,7,8-PeCDF	(0.03)	0.06	0.02	0.3	0.009
	PeCDFs	0.51	-	-	-	
	1,2,3,4,7,8-HxCDF	(0.06)	0.11	0.04	0.1	0.006
	1,2,3,6,7,8-HxCDF	(0.05)	0.11	0.04	0.1	0.005
	1,2,3,7,8,9-HxCDF	N.D.	0.11	0.04	0.1	0.002
	2,3,4,6,7,8-HxCDF	0.15	0.11	0.04	0.1	0.015
	HxCDFs	0.68	-	-	-	
	1,2,3,4,6,7,8-HpCDF	0.46	0.11	0.04	0.01	0.0046
	1,2,3,4,7,8,9-HpCDF	(0.09)	0.11	0.04	0.01	0.0009
	HpCDFs	0.87	-	-	-	
	OCDF	0.46	0.15	0.05	0.0003	0.000138
	Total PCDFs	2.7	-	-	-	0.045
Total (PCDDs + PCDFs)		8.0	-	-	-	0.098
coplanar-PCBs	3,4,4',5-TeCB	N.D.	0.11	0.04	0.0003	0.000006
	3,3',4,4'-TeCB	(0.07)	0.11	0.04	0.0001	0.000007
	3,3',4,4',5-PeCB	N.D.	0.11	0.04	0.1	0.002
	3,3',4,4',5,5'-HxCB	N.D.	0.11	0.04	0.03	0.0006
	Non-ortho PCBs	0.07	-	-	-	0.0026
	2',3,4,4',5-PeCB	N.D.	0.11	0.04	0.00003	0.0000006
	2,3',4,4',5-PeCB	0.33	0.11	0.04	0.00003	0.0000099
	2,3,3',4,4'-PeCB	0.14	0.11	0.04	0.00003	0.0000042
	2,3,4,4',5-PeCB	N.D.	0.11	0.04	0.00003	0.0000006
	2,3',4,4',5,5'-HxCB	N.D.	0.11	0.04	0.00003	0.0000006
	2,3,3',4,4',5-HxCB	(0.07)	0.11	0.04	0.00003	0.0000021
	2,3,3',4,4',5'-HxCB	N.D.	0.11	0.04	0.00003	0.0000006
	2,3,3',4,4',5,5'-HpCB	(0.05)	0.11	0.04	0.00003	0.0000015
	Mono-ortho PCBs	0.59	-	-	-	0.000020
Total coplanar-PCBs		0.66	-	-	-	0.0026
Total (PCDDs + PCDF + coplanar-PCBs)		8.7	-	-	-	0.10

1. The values of 1,2,3,7,8-PeCDF and 1,2,3,4,7,8-HxCDF include those of 1,2,3,4,8-PeCDF and 1,2,3,4,7,9-HxCDF, respectively, because of inability to resolve them on chromatogram.
2. "()" in "measured concentration" column means the value between quantification limit and detection limit.
3. "N.D." in "measured concentration" column means "not detected".
4. The value of TEF is based on WHO-TEF (2006).
5. TEQ was calculated by using either the value of "measured concentration" when they could be detected or the half value of "detection limit" when they could not detected.

Table 1C. Particulate dioxins before photocatalysis (Experiment 2).

	Dioxins	measured concentration (pg/m^3)	quantification limit of sample (pg/m^3)	detection limit of sample (pg/m^3)	toxic equivalency factor (TEF)	toxic equivalent (TEQ) (pg-TEQ/m^3)
PCDDs	1,3,6,8-TeCDD	0.18	0.05	0.02	-	
	1,3,7,9-TeCDD	0.07	0.05	0.02	-	
	2,3,7,8-TeCDD	(0.03)	0.05	0.02	1	0.03
	TeCDDs	0.47	-	-	-	
	1,2,3,7,8-PeCDD	0.07	0.06	0.02	1	0.07
	PeCDDs	1.0	-	-	-	
	1,2,3,4,7,8-HxCDD	(0.05)	0.11	0.04	0.1	0.005
	1,2,3,6,7,8-HxCDD	0.13	0.11	0.04	0.1	0.013
	1,2,3,7,8,9-HxCDD	(0.09)	0.11	0.04	0.1	0.009
	HxCDDs	2.1	-	-	-	
	1,2,3,4,6,7,8-HpCDD	2.3	0.11	0.04	0.01	0.023
	HpCDDs	4.8	-	-	-	
	OCDD	10	0.13	0.04	0.0003	0.0030
	Total PCDDs	18	-	-	-	0.15
PCDFs	1,2,7,8-TeCDF	0.08	0.06	0.02	-	
	2,3,7,8-TeCDF	(0.04)	0.06	0.02	0.1	0.004
	TeCDFs	2.6	-	-	-	
	1,2,3,7,8-PeCDF	0.25	0.06	0.02	0.03	0.0075
	2,3,4,7,8-PeCDF	0.29	0.06	0.02	0.3	0.087
	PeCDFs	4.2	-	-	-	
	1,2,3,4,7,8-HxCDF	0.34	0.11	0.04	0.1	0.034
	1,2,3,6,7,8-HxCDF	0.39	0.11	0.04	0.1	0.039
	1,2,3,7,8,9-HxCDF	N.D.	0.11	0.04	0.1	0.002
	2,3,4,6,7,8-HxCDF	0.64	0.11	0.04	0.1	0.064
	HxCDFs	4.4	-	-	-	
	1,2,3,4,6,7,8-HpCDF	1.8	0.11	0.04	0.01	0.018
	1,2,3,4,7,8,9-HpCDF	0.30	0.11	0.04	0.01	0.0030
	HpCDFs	3.3	-	-	-	
	OCDF	1.3	0.15	0.05	0.0003	0.00039
	Total PCDFs	16	-	-	-	0.26
Total (PCDDs + PCDFs)		34	-	-	-	0.41
coplanar-PCBs	3,4,4',5-TeCB	(0.08)	0.11	0.04	0.0003	0.000024
	3,3',4,4'-TeCB	0.25	0.11	0.04	0.0001	0.000025
	3,3',4,4',5-PeCB	0.38	0.11	0.04	0.1	0.038
	3,3',4,4',5,5'-HxCB	0.25	0.11	0.04	0.03	0.0075
	Non-ortho PCBs	0.96	-	-	-	0.046
	2',3,4,4',5-PeCB	(0.06)	0.11	0.04	0.00003	0.0000018
	2,3',4,4',5-PeCB	2.3	0.11	0.04	0.00003	0.000069
	2,3,3',4,4'-PeCB	1.1	0.11	0.04	0.00003	0.000033
	2,3,4,4',5-PeCB	0.12	0.11	0.04	0.00003	0.0000036
	2,3',4,4',5,5'-HxCB	0.24	0.11	0.04	0.00003	0.0000072
	2,3,3',4,4',5-HxCB	0.69	0.11	0.04	0.00003	0.0000207
	2,3,3',4,4',5'-HxCB	0.26	0.11	0.04	0.00003	0.0000078
	2,3,3',4,4',5,5'-HpCB	0.47	0.11	0.04	0.00003	0.0000141
	Mono-ortho PCBs	5.2	-	-	-	0.00016
Total coplanar-PCBs		6.2	-	-	-	0.046
Total (PCDDs + PCDFs + coplanar-PCBs)		40	-	-	-	0.46

1. The values of 1,2,3,7,8-PeCDF and 1,2,3,4,7,8-HxCDF include those of 1,2,3,4,8-PeCDF and 1,2,3,4,7,9-HxCDF, respectively, because of inability to resolve them on chromatogram.
2. "()" in "measured concentration" column means the value between quantification limit and detection limit.
3. "N.D." in "measured concentration" column means "not detected".
4. The value of TEF is based on WHO-TEF (2006).
5. TEQ was calculated by using either the value of "measured concentration" when they could be detected or the half value of "detection limit" when they could not detected.

Table 1D. Particulate dioxins removed after photocatalysis (Experiment 2).

	Dioxins	measured concentration (pg/m^3)	quantification limit of sample (pg/m^3)	detection limit of sample (pg/m^3)	toxic equivalency factor (TEF)	toxic equivalent (TEQ) ($pg\text{-}TEQ/m^3$)
PCDDs	1,3,6,8-TeCDD	(0.03)	0.05	0.02	-	
	1,3,7,9-TeCDD	N.D.	0.05	0.02	-	
	2,3,7,8-TeCDD	N.D.	0.05	0.02	1	0.01
	TeCDDs	0.03	-	-	-	
	1,2,3,7,8-PeCDD	N.D.	0.06	0.02	1	0.01
	PeCDDs	0.09	-	-	-	
	1,2,3,4,7,8-HxCDD	N.D.	0.11	0.04	0.1	0.002
	1,2,3,6,7,8-HxCDD	N.D.	0.11	0.04	0.1	0.002
	1,2,3,7,8,9-HxCDD	N.D.	0.11	0.04	0.1	0.002
	HxCDDs	0.30	-	-	-	
	1,2,3,4,6,7,8-HpCDD	0.49	0.11	0.04	0.01	0.0049
	HpCDDs	1.0	-	-	-	
	OCDD	2.4	0.13	0.04	0.0003	0.00072
	Total PCDDs	3.8	-	-	-	0.032
PCDFs	1,2,7,8-TeCDF	N.D.	0.06	0.02	-	
	2,3,7,8-TeCDF	N.D.	0.06	0.02	0.1	0.001
	TeCDFs	0.39	-	-	-	
	1,2,3,7,8-PeCDF	(0.05)	0.06	0.02	0.03	0.0015
	2,3,4,7,8-PeCDF	(0.04)	0.06	0.02	0.3	0.012
	PeCDFs	0.65	-	-	-	
	1,2,3,4,7,8-HxCDF	(0.06)	0.11	0.04	0.1	0.006
	1,2,3,6,7,8-HxCDF	(0.09)	0.11	0.04	0.1	0.009
	1,2,3,7,8,9-HxCDF	N.D.	0.11	0.04	0.1	0.002
	2,3,4,6,7,8-HxCDF	0.14	0.11	0.04	0.1	0.014
	HxCDFs	0.77	-	-	-	
	1,2,3,4,6,7,8-HpCDF	0.46	0.11	0.04	0.01	0.0046
	1,2,3,4,7,8,9-HpCDF	(0.08)	0.11	0.04	0.01	0.0008
	HpCDFs	0.86	-	-	-	
	OCDF	0.36	0.15	0.05	0.0003	0.000108
	Total PCDFs	3.0	-	-	-	0.051
Total (PCDDs + PCDFs)		6.9	-	-	-	0.083
coplanar-PCBs	3,4,4',5-TeCB	N.D.	0.11	0.04	0.0003	0.000006
	3,3',4,4'-TeCB	(0.07)	0.11	0.04	0.0001	0.000007
	3,3',4,4',5-PeCB	(0.06)	0.11	0.04	0.1	0.006
	3,3',4,4',5,5'-HxCB	N.D.	0.11	0.04	0.03	0.0006
	Non-ortho PCBs	0.13	-	-	-	0.0066
	2',3,4,4',5-PeCB	N.D.	0.11	0.04	0.00003	0.0000006
	2,3',4,4',5-PeCB	0.28	0.11	0.04	0.00003	0.0000084
	2,3,3',4,4'-PeCB	0.14	0.11	0.04	0.00003	0.0000042
	2,3,4,4',5-PeCB	N.D.	0.11	0.04	0.00003	0.0000006
	2,3',4,4',5,5'-HxCB	N.D.	0.11	0.04	0.00003	0.0000006
	2,3,3',4,4',5-HxCB	(0.09)	0.11	0.04	0.00003	0.0000027
	2,3,3',4,4',5'-HxCB	N.D.	0.11	0.04	0.00003	0.0000006
	2,3,3',4,4',5,5'-HpCB	(0.05)	0.11	0.04	0.00003	0.0000015
	Mono-ortho PCBs	0.56	-	-	-	0.000019
Total coplanar-PCBs		0.69	-	-	-	0.0066
Total (PCDDs + PCDFs + coplanar-PCBs)		7.5	-	-	-	0.089

1. The values of 1,2,3,7,8-PeCDF and 1,2,3,4,7,8-HxCDF include those of 1,2,3,4,8-PeCDF and 1,2,3,4,7,9-HxCDF, respectively, because of inability to resolve them on chromatogram.
2. "()" in "measured concentration" column means the value between quantification limit and detection limit.
3. "N.D." in "measured concentration" column means "not detected".
4. The value of TEF is based on WHO-TEF (2006).
5. TEQ was calculated by using either the value of "measured concentration" when they could be detected or the half value of "detection limit" when they could not detected.

Table 2A. Gaseous dioxins before photocatalysis (Experiment 1).

	Dioxins	measured concentration (pg/m^3)	quantification limit of sample (pg/m^3)	detection limit of sample (pg/m^3)	toxic equivalency factor (TEF)	toxic equivalent (TEQ) (pg-TEQ/m^3)
PCDDs	1,3,6,8-TeCDD	0.36	0.05	0.02	-	
	1,3,7,9-TeCDD	0.14	0.05	0.02	-	
	2,3,7,8-TeCDD	N.D.	0.05	0.02	1	0.01
	TeCDDs	0.75	-	-	-	
	1,2,3,7,8-PeCDD	N.D.	0.06	0.02	1	0.01
	PeCDDs	0.23	-	-	-	
	1,2,3,4,7,8-HxCDD	N.D.	0.11	0.04	0.1	0.002
	1,2,3,6,7,8-HxCDD	N.D.	0.11	0.04	0.1	0.002
	1,2,3,7,8,9-HxCDD	N.D.	0.11	0.04	0.1	0.002
	HxCDDs	N.D.	-	-	-	
	1,2,3,4,6,7,8-HpCDD	N.D.	0.11	0.04	0.01	0.0002
	HpCDDs	0.07	-	-	-	
	OCDD	0.22	0.13	0.04	0.0003	0.000066
	Total PCDDs	1.3	-	-	-	0.026
PCDFs	1,2,7,8-TeCDF	0.15	0.06	0.02	-	
	2,3,7,8-TeCDF	0.09	0.06	0.02	0.1	0.009
	TeCDFs	7.2	-	-	-	
	1,2,3,7,8-PeCDF	0.17	0.06	0.02	0.03	0.0051
	2,3,4,7,8-PeCDF	(0.04)	0.06	0.02	0.3	0.012
	PeCDFs	2.4	-	-	-	
	1,2,3,4,7,8-HxCDF	N.D.	0.11	0.04	0.1	0.002
	1,2,3,6,7,8-HxCDF	N.D.	0.11	0.04	0.1	0.002
	1,2,3,7,8,9-HxCDF	N.D.	0.11	0.04	0.1	0.002
	2,3,4,6,7,8-HxCDF	N.D.	0.11	0.04	0.1	0.002
	HxCDFs	N.D.	-	-	-	
	1,2,3,4,6,7,8-HpCDF	N.D.	0.11	0.04	0.01	0.0002
	1,2,3,4,7,8,9-HpCDF	N.D.	0.11	0.04	0.01	0.0002
	HpCDFs	N.D.	-	-	-	
	OCDF	N.D.	0.15	0.05	0.0003	0.0000075
	Total PCDFs	9.6	-	-	-	0.035
Total (PCDDs + PCDFs)		11	-	-	-	0.061
coplanar-PCBs	3,4,4',5-TeCB	0.55	0.11	0.04	0.0003	0.000165
	3,3',4,4'-TeCB	1.8	0.11	0.04	0.0001	0.00018
	3,3',4,4',5-PeCB	0.59	0.11	0.04	0.1	0.059
	3,3',4,4',5,5'-HxCB	N.D.	0.11	0.04	0.03	0.0006
	Non-ortho PCBs	2.9	-	-	-	0.060
	2',3,4,4',5-PeCB	0.44	0.11	0.04	0.00003	0.0000132
	2,3',4,4',5-PeCB	14	0.11	0.04	0.00003	0.00042
	2,3,3',4,4'-PeCB	4.7	0.11	0.04	0.00003	0.000141
	2,3,4,4',5-PeCB	0.74	0.11	0.04	0.00003	0.0000222
	2,3',4,4',5,5'-HxCB	0.39	0.11	0.04	0.00003	0.0000117
	2,3,3',4,4',5-HxCB	0.86	0.11	0.04	0.00003	0.0000258
	2,3,3',4,4',5'-HxCB	0.31	0.11	0.04	0.00003	0.0000093
	2,3,3',4,4',5,5'-HpCB	(0.06)	0.11	0.04	0.00003	0.0000018
	Mono-ortho PCBs	22	-	-	-	0.00065
Total coplanar-PCBs		24	-	-	-	0.061
Total (PCDDs + PCDF + coplanar-PCBs)		35	-	-	-	0.12

1. The values of 1,2,3,7,8-PeCDF and 1,2,3,4,7,8-HxCDF include those of 1,2,3,4,8-PeCDF and 1,2,3,4,7,9-HxCDF, respectively, because of inability to resolve them on chromatogram.
2. "()" in "measured concentration" column means the value between quantification limit and detection limit.
3. "N.D." in "measured concentration" column means "not detected".
4. The value of TEF is based on WHO-TEF (2006).
5. TEQ was calculated by using either the value of "measured concentration" when they could be detected or the half value of "detection limit" when they could not detected.

Table 2B. Gaseous dioxins removed after photocatalysis (Experiment 1).

	Dioxins	measured concentration (pg/m^3)	quantification limit of sample (pg/m^3)	detection limit of sample (pg/m^3)	toxic equivalency factor (TEF)	toxic equivalent (TEQ) (pg-TEQ/m^3)
PCDDs	1,3,6,8-TeCDD	N.D.	0.05	0.02	-	
	1,3,7,9-TeCDD	N.D.	0.05	0.02	-	
	2,3,7,8-TeCDD	N.D.	0.05	0.02	1	0.01
	TeCDDs	N.D.	-	-	-	
	1,2,3,7,8-PeCDD	N.D.	0.06	0.02	1	0.01
	PeCDDs	N.D.	-	-	-	
	1,2,3,4,7,8-HxCDD	N.D.	0.11	0.04	0.1	0.002
	1,2,3,6,7,8-HxCDD	N.D.	0.11	0.04	0.1	0.002
	1,2,3,7,8,9-HxCDD	N.D.	0.11	0.04	0.1	0.002
	HxCDDs	N.D.	-	-	-	
	1,2,3,4,6,7,8-HpCDD	N.D.	0.11	0.04	0.01	0.0002
	HpCDDs	N.D.	-	-	-	
	OCDD	(0.07)	0.13	0.04	0.0003	0.000021
	Total PCDDs	0.07	-	-	-	0.026
PCDFs	1,2,7,8-TeCDF	N.D.	0.06	0.02	-	
	2,3,7,8-TeCDF	N.D.	0.06	0.02	0.1	0.001
	TeCDFs	N.D.	-	-	-	
	1,2,3,7,8-PeCDF	N.D.	0.06	0.02	0.03	0.0003
	2,3,4,7,8-PeCDF	N.D.	0.06	0.02	0.3	0.003
	PeCDFs	N.D.	-	-	-	
	1,2,3,4,7,8-HxCDF	N.D.	0.11	0.04	0.1	0.002
	1,2,3,6,7,8-HxCDF	N.D.	0.11	0.04	0.1	0.002
	1,2,3,7,8,9-HxCDF	N.D.	0.11	0.04	0.1	0.002
	2,3,4,6,7,8-HxCDF	N.D.	0.11	0.04	0.1	0.002
	HxCDFs	N.D.	-	-	-	
	1,2,3,4,6,7,8-HpCDF	N.D.	0.11	0.04	0.01	0.0002
	1,2,3,4,7,8,9-HpCDF	N.D.	0.11	0.04	0.01	0.0002
	HpCDFs	N.D.	-	-	-	
	OCDF	N.D.	0.15	0.05	0.0003	0.0000075
	Total PCDFs	N.D.	-	-	-	0.013
Total (PCDDs + PCDFs)		0.07	-	-	-	0.039
coplanar-PCBs	3,4,4',5-TeCB	N.D.	0.11	0.04	0.0003	0.000006
	3,3',4,4'-TeCB	0.24	0.11	0.04	0.0001	0.000024
	3,3',4,4',5-PeCB	N.D.	0.11	0.04	0.1	0.002
	3,3',4,4',5,5'-HxCB	N.D.	0.11	0.04	0.03	0.0006
	Non-ortho PCBs	0.24	-	-	-	0.0026
	2',3,4,4',5-PeCB	(0.05)	0.11	0.04	0.00003	0.0000015
	2,3',4,4',5-PeCB	1.8	0.11	0.04	0.00003	0.000054
	2,3,3',4,4'-PeCB	0.65	0.11	0.04	0.00003	0.0000195
	2,3,4,4',5-PeCB	(0.09)	0.11	0.04	0.00003	0.0000027
	2,3',4,4',5,5'-HxCB	N.D.	0.11	0.04	0.00003	0.0000006
	2,3,3',4,4',5-HxCB	(0.08)	0.11	0.04	0.00003	0.0000024
	2,3,3',4,4',5'-HxCB	N.D.	0.11	0.04	0.00003	0.0000006
	2,3,3',4,4',5,5'-HpCB	N.D.	0.11	0.04	0.00003	0.0000006
	Mono-ortho PCBs	2.7	-	-	-	0.000082
Total coplanar-PCBs		2.9	-	-	-	0.0027
Total (PCDDs + PCDF + coplanar-PCBs)		3.0	-	-	-	0.042

1. The values of 1,2,3,7,8-PeCDF and 1,2,3,4,7,8-HxCDF include those of 1,2,3,4,8-PeCDF and 1,2,3,4,7,9-HxCDF, respectively, because of inability to resolve them on chromatogram.
2. "()" in "measured concentration" column means the value between quantification limit and detection limit.
3. "N.D." in "measured concentration" column means "not detected".
4. The value of TEF is based on WHO-TEF (2006).
5. TEQ was calculated by using either the value of "measured concentration" when they could be detected or the half value of "detection limit" when they could not detected.

Table 2C. Gaseous dioxins before photocatalysis (Experiment 2).

	Dioxins	measured concentration (pg/m^3)	quantification limit of sample (pg/m^3)	detection limit of sample (pg/m^3)	toxic equivalency factor (TEF)	toxic equivalent (TEQ) ($pg\text{-}TEQ/m^3$)
PCDDs	1,3,6,8-TeCDD	0.19	0.05	0.02	-	
	1,3,7,9-TeCDD	0.08	0.05	0.02	-	
	2,3,7,8-TeCDD	N.D.	0.05	0.02	1	0.01
	TeCDDs	0.38	-	-	-	
	1,2,3,7,8-PeCDD	N.D.	0.06	0.02	1	0.01
	PeCDDs	0.09	-	-	-	
	1,2,3,4,7,8-HxCDD	N.D.	0.11	0.04	0.1	0.002
	1,2,3,6,7,8-HxCDD	N.D.	0.11	0.04	0.1	0.002
	1,2,3,7,8,9-HxCDD	N.D.	0.11	0.04	0.1	0.002
	HxCDDs	N.D.	-	-	-	
	1,2,3,4,6,7,8-HpCDD	N.D.	0.11	0.04	0.01	0.0002
	HpCDDs	N.D.	-	-	-	
	OCDD	N.D.	0.13	0.04	0.0003	0.000006
	Total PCDDs	0.47	-	-	-	0.026
PCDFs	1,2,7,8-TeCDF	0.11	0.06	0.02	-	
	2,3,7,8-TeCDF	(0.04)	0.06	0.02	0.1	0.004
	TeCDFs	4.3	-	-	-	
	1,2,3,7,8-PeCDF	0.12	0.06	0.02	0.03	0.0036
	2,3,4,7,8-PeCDF	(0.03)	0.06	0.02	0.3	0.009
	PeCDFs	1.4	-	-	-	
	1,2,3,4,7,8-HxCDF	N.D.	0.11	0.04	0.1	0.002
	1,2,3,6,7,8-HxCDF	N.D.	0.11	0.04	0.1	0.002
	1,2,3,7,8,9-HxCDF	N.D.	0.11	0.04	0.1	0.002
	2,3,4,6,7,8-HxCDF	N.D.	0.11	0.04	0.1	0.002
	HxCDFs	N.D.	-	-	-	
	1,2,3,4,6,7,8-HpCDF	N.D.	0.11	0.04	0.01	0.0002
	1,2,3,4,7,8,9-HpCDF	N.D.	0.11	0.04	0.01	0.0002
	HpCDFs	N.D.	-	-	-	
	OCDF	N.D.	0.15	0.05	0.0003	0.0000075
	Total PCDFs	5.7	-	-	-	0.025
Total (PCDDs + PCDFs)		6.2	-	-	-	0.051
coplanar-PCBs	3,4,4',5-TeCB	0.32	0.11	0.04	0.0003	0.000096
	3,3',4,4'-TeCB	0.78	0.11	0.04	0.0001	0.000078
	3,3',4,4',5-PeCB	0.36	0.11	0.04	0.1	0.036
	3,3',4,4',5,5'-HxCB	N.D.	0.11	0.04	0.03	0.0006
	Non-ortho PCBs	1.5	-	-	-	0.037
	2',3,4,4',5-PeCB	0.19	0.11	0.04	0.00003	0.0000057
	2,3',4,4',5-PeCB	5.4	0.11	0.04	0.00003	0.000162
	2,3,3',4,4'-PeCB	2.0	0.11	0.04	0.00003	0.000060
	2,3,4,4',5-PeCB	0.35	0.11	0.04	0.00003	0.0000105
	2,3',4,4',5,5'-HxCB	0.19	0.11	0.04	0.00003	0.0000057
	2,3,3',4,4',5-HxCB	0.39	0.11	0.04	0.00003	0.0000117
	2,3,3',4,4',5'-HxCB	0.17	0.11	0.04	0.00003	0.0000051
	2,3,3',4,4',5,5'-HpCB	(0.04)	0.11	0.04	0.00003	0.0000012
	Mono-ortho PCBs	8.7	-	-	-	0.00026
Total coplanar-PCBs		10	-	-	-	0.037
Total (PCDDs + PCDFs + coplanar-PCBs)		16	-	-	-	0.088

1. The values of 1,2,3,7,8-PeCDF and 1,2,3,4,7,8-HxCDF include those of 1,2,3,4,8-PeCDF and 1,2,3,4,7,9-HxCDF, respectively, because of inability to resolve them on chromatogram.
2. "()" in "measured concentration" column means the value between quantification limit and detection limit.
3. "N.D." in "measured concentration" column means "not detected"..
4. The value of TEF is based on WHO-TEF (2006).
5. TEQ was calculated by using either the value of "measured concentration" when they could be detected or the half value of "detection limit" when they could not detected.

Table 2D. Gaseous dioxins removed after photocatalysis (Experiment 2).

	Dioxins	measured concentration (pg/m^3)	quantification limit of sample (pg/m^3)	detection limit of sample (pg/m^3)	toxic equivalency factor (TEF)	toxic equivalent (TEQ) ($pg\text{-}TEQ/m^3$)
PCDDs	1,3,6,8-TeCDD	(0.03)	0.05	0.02	-	
	1,3,7,9-TeCDD	N.D.	0.05	0.02	-	
	2,3,7,8-TeCDD	N.D.	0.05	0.02	1	0.01
	TeCDDs	0.03	-	-	-	
	1,2,3,7,8-PeCDD	N.D.	0.06	0.02	1	0.01
	PeCDDs	N.D.	-	-	-	
	1,2,3,4,7,8-HxCDD	N.D.	0.11	0.04	0.1	0.002
	1,2,3,6,7,8-HxCDD	N.D.	0.11	0.04	0.1	0.002
	1,2,3,7,8,9-HxCDD	N.D.	0.11	0.04	0.1	0.002
	HxCDDs	N.D.	-	-	-	
	1,2,3,4,6,7,8-HpCDD	(0.06)	0.11	0.04	0.01	0.0006
	HpCDDs	0.11	-	-	-	
	OCDD	0.22	0.13	0.04	0.0003	0.000066
	Total PCDDs	0.36	-	-	-	0.027
PCDFs	1,2,7,8-TeCDF	N.D.	0.06	0.02	-	
	2,3,7,8-TeCDF	N.D.	0.06	0.02	0.1	0.001
	TeCDFs	0.07	-	-	-	
	1,2,3,7,8-PeCDF	N.D.	0.06	0.02	0.03	0.0003
	2,3,4,7,8-PeCDF	N.D.	0.06	0.02	0.3	0.003
	PeCDFs	0.03	-	-	-	
	1,2,3,4,7,8-HxCDF	N.D.	0.11	0.04	0.1	0.002
	1,2,3,6,7,8-HxCDF	N.D.	0.11	0.04	0.1	0.002
	1,2,3,7,8,9-HxCDF	N.D.	0.11	0.04	0.1	0.002
	2,3,4,6,7,8-HxCDF	N.D.	0.11	0.04	0.1	0.002
	HxCDFs	N.D.	-	-	-	
	1,2,3,4,6,7,8-HpCDF	N.D.	0.11	0.04	0.01	0.0002
	1,2,3,4,7,8,9-HpCDF	N.D.	0.11	0.04	0.01	0.0002
	HpCDFs	N.D.	-	-	-	
	OCDF	N.D.	0.15	0.05	0.0003	0.0000075
	Total PCDFs	0.10	-	-	-	0.013
Total (PCDDs + PCDFs)		0.46	-	-	-	0.039
coplanar-PCBs	3,4,4',5-TeCB	N.D.	0.11	0.04	0.0003	0.000006
	3,3',4,4'-TeCB	0.15	0.11	0.04	0.0001	0.000015
	3,3',4,4',5-PeCB	N.D.	0.11	0.04	0.1	0.002
	3,3',4,4',5,5'-HxCB	N.D.	0.11	0.04	0.03	0.0006
	Non-ortho PCBs	0.15	-	-	-	0.0026
	2',3,4,4',5-PeCB	N.D.	0.11	0.04	0.00003	0.0000006
	2,3',4,4',5-PeCB	1.4	0.11	0.04	0.00003	0.000042
	2,3,3',4,4'-PeCB	0.58	0.11	0.04	0.00003	0.0000174
	2,3,4,4',5-PeCB	(0.06)	0.11	0.04	0.00003	0.0000018
	2,3',4,4',5,5'-HxCB	(0.05)	0.11	0.04	0.00003	0.0000015
	2,3,3',4,4',5-HxCB	0.13	0.11	0.04	0.00003	0.0000039
	2,3,3',4,4',5'-HxCB	N.D.	0.11	0.04	0.00003	0.0000006
	2,3,3',4,4',5,5'-HpCB	N.D.	0.11	0.04	0.00003	0.0000006
	Mono-ortho PCBs	2.2	-	-	-	0.000068
Total coplanar-PCBs		2.4	-	-	-	0.0027
Total (PCDDs + PCDFs + coplanar-PCBs)		2.8	-	-	-	0.042

1. The values of 1,2,3,7,8-PeCDF and 1,2,3,4,7,8-HxCDF include those of 1,2,3,4,8-PeCDF and 1,2,3,4,7,9-HxCDF, respectively, because of inability to resolve them on chromatogram.
2. "()" in "measured concentration" column means the value between quantification limit and detection limit.
3. "N.D." in "measured concentration" column means "not detected".
4. The value of TEF is based on WHO-TEF (2006).
5. TEQ was calculated by using either the value of "measured concentration" when they could be detected or the half value of "detection limit" when they could not detected.

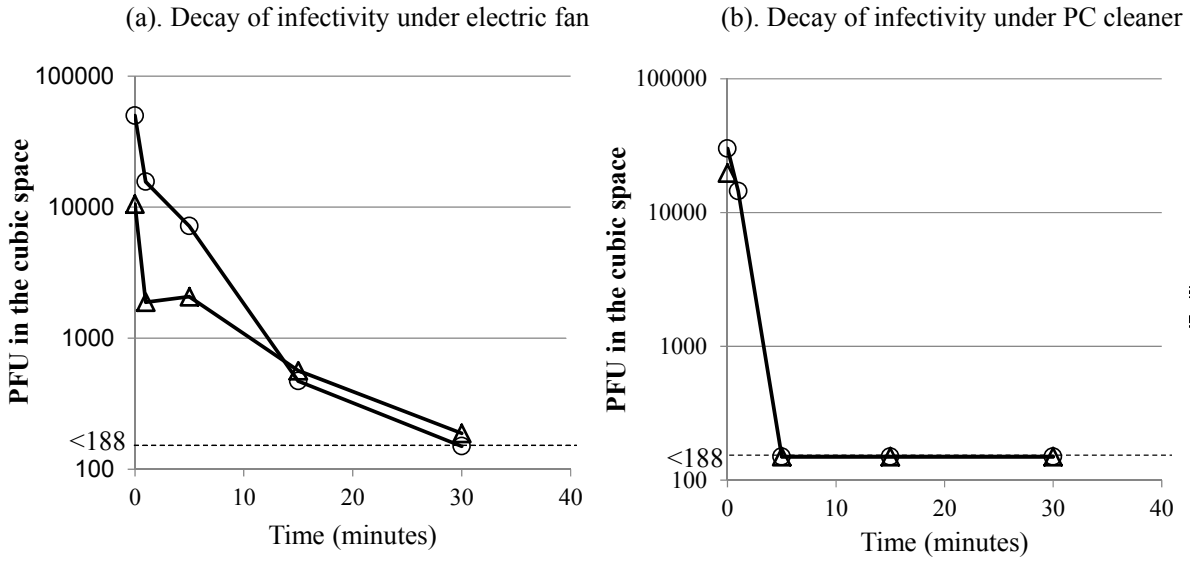

Fig. 4. Stability and decay of aerosol-associated infectivity of influenza virus in the closed space (a) and its inactivation by the photocatalytic air cleaner (b). Influenza virus was nebulized into the space, and 40-L volumes of air were serially transferred from bag A through the cubic space to bag B, and the infectivity of the air in bag B was determined. During the experiment, the air in the space was circulated by an electric fan or by the fan in the photocatalytic air cleaner. Two experimental results (O and ∆) were shown in the figures. The figures are modified from the original figures (Shiraki *et al*., 2011).

When tobacco tar and so on sticks to the ceramic, the photocatalytic reaction is blocked by the blockade of ultraviolet light to the surface. This can be removed by the sunlight in the place where there is no smoke of tobacco. Thus photocatalytic ceramic is a stable, durable, and reusable material.

The importance of aerosol-associated influenza infection has been reported experimentally and clinically as the major and efficient route of transmission, especially in closed public spaces with low ventilation. Aerosol of 1–3 μm is produced directly or by evaporation of droplets exhaled in a cough or sneeze of a patient infected with influenza and preferentially deposited in the lower airways of the lung (Heyder, 1986; Knight, 1980; Isaacs and Martonen, 2005), resulting in efficient transmission. Thus, the aerosol produced by sneezes and coughs as well as the continuous tidal expiration of patients may be an important source for the transmission of influenza in a closed space with inefficient ventilation. Aerosol associated with infectivity may accumulate in a closed space due to continuous production of aerosol by sneezes and coughs as well as tidal expiration, and continuous production of the aerosol by sneezes or coughs for three hours resulted in the efficient spread of infection to 72% of 54 passengers in an airplane (Moser *et al.*, 1979).

We developed an assay system to measure the aerosol-associated infectivity of influenza virus and confirmed the persistence of aerosol-associated infectivity in the air of the closed space. The aerosol-associated infectivity of influenza virus was detectable for up to 30 minutes in the closed space after it was once filled with infectious aerosol. Continuous production of aerosol-associated influenza by sneezes and coughs as well as tidal expiration may accumulate in the closed space and result in the efficient spread of infection of influenza in public spaces, especially in the poor ventilation condition. The aerosol-associated infectivity of influenza virus was efficiently and quickly inactivated by the photocatalytic air cleaner, which emitted superoxide anions and hydroxyl radicals as the disinfecting agent. The surface area of titanium-coated ceramic was produced in a porous form to increase the surface area producing activated oxygen and ventilation efficiency of the photocatalytic air cleaner.

In this study we established a porous ceramic system for photocatalysis to decompose organic chemicals including acetaldehyde and dioxins and inactivate aerosol-associated influenza virus infectivity and applied it as a photocatalytic air cleaner consisting of the titanium-coated porous ceramic boards under black light. This study showed the usefulness and importance in clearing harmful organic chemicals and aerosol-associated influenza in suppressing its outbreak by the photocatalytic air cleaner.

ACKNOWLEDGEMENTS

We thank Ms. Katherine Ono for editing the manuscript. This study was partly supported by OTA Inc., Tokyo, Japan.

REFERENCES

Alford, R.H., Kasel, J.A., Gerone, P.J. and Knight, V. (1966). Human Influenza Resulting from Aerosol Inhalation. *Proc. Soc. Exp. Biol. Med.* 122: 800–804.

Andrewes, C.H. and Glover, R.E. (1941). Spread of Infection from the Respiratory Tract of the Ferret: I. Transmission of Influenza A Virus. *Br. J. Exp. Pathol.* 22: 1129–1130.

Asahi, R., Morikawa, T., Ohwaki, T., Aoki, K. and Taga, Y. (2001). Visible-Light Photocatalysis in Nitrogen-Doped Titanium Oxides. *Science* 293: 269–271.

Chen, S.C., Chio, C.P., Jou, L.J. and Liao, C.M. (2009).

Viral Kinetics and Exhaled Droplet Size Affect Indoor Transmission Dynamics of Influenza Infection. *Indoor Air* 19: 401–413.

Couch, R.B., Douglas, R.G., Jr., Fedson, D.S. and Kasel, J.A. (1971). Correlated Studies of a Recombinant Influenza-Virus Vaccine. 3. Protection against Experimental Influenza in Man. *J. Infect. Dis.* 124: 473–480.

Couch, R.B. and Kasel, J.A. (1983). Immunity to Influenza in Man. *Annu. Rev. Microbiol.* 37: 529–549.

Fabian, P., McDevitt, J.J., DeHaan, W.H., Fung, R.O., Cowling, B.J., Chan, K.H., Leung, G.M. and Milton, D.K. (2008). Influenza Virus in Human Exhaled Breath: An Observational Study. *PLoS ONE* 3: e2691.

Fujishima, A. and Honda, K. (1972). Electrochemical Photolysis of Water at a Semiconductor Electrode. *Nature* 238: 37–38.

Furuta, Y., Takahashi, K., Fukuda, Y., Kuno, M., Kamiyama, T., Kozaki, K., Nomura, N., Egawa, H., Minami, S., Watanabe, Y., Narita, H. and Shiraki, K. (2002). In Vitro and in Vivo Activities of Anti-Influenza Virus Compound T-705. *Antimicrob. Agents Chemother.* 46: 977–981.

Furuta, Y., Takahashi, K., Kuno-Maekawa, M., Sangawa, H., Uehara, S., Kozaki, K., Nomura, N., Egawa, H. and Shiraki, K. (2005). Mechanism of Action of T-705 against Influenza Virus. *Antimicrob. Agents Chemother.* 49: 981–986.

Furuta, Y., Takahashi, K., Shiraki, K., Sakamoto, K., Smee, D.F., Barnard, D.L., Gowen, B.B., Julander, J.G. and Morrey, J.D.(2009). T-705 (favipiravir) and Related Compounds: Novel Broad-Spectrum Inhibitors of RNA Viral Infections. *Antiviral Res.* 82: 95–102.

Goldmann, D.A. (2000). Transmission of Viral Respiratory Infections in the Home. *Pediatr. Infect. Dis. J.* 19 S97–102.

Guglielmotti, D.M., Mercanti, D.J., Reinheimer, J.A. and Quiberoni Adel, L. (2011). Review: Efficiency of Physical and Chemical Treatments on the Inactivation of Dairy Bacteriophages. *Front. Microbiol.* 2: 282.

Heyder, J., Gebherat, J., Rudolf, G., Schiller, C.F. and Stahlhofen, W. (1986). Deposition of Particles in the Human Respiratory Tract in the Size Range 0.005-15 mm. *J. Arerosol Sci.* 17: 811–825.

Huang, X., Yuan, J., Shi, J. and Shangguan, W. (2009). Ozone-Assisted Photocatalytic Oxidation of Gaseous Acetaldehyde on TiO_2/H-ZSM-5 Catalysts. *J. Hazard. Mater.* 171: 827–832.

Isaacs, K.K. and Martonen, T.B. (2005). Particle Deposition in Children's Lungs: Theory and Experiment. *J. Aerosol Med.* 18: 337–353.

Knight, V. (1980). Viruses as Agents of Airborne Contagion. *Ann. N.Y. Acad. Sci.* 353: 147–156.

Kurokawa, M., Imakita, M., Kumeda, C.A. and Shiraki, K. (1996a). Cascade of Fever Production in Mice Infected with Influenza Virus. *J. Med. Virol.* 50: 152–158.

Kurokawa, M., Ohyama, H., Hozumi, T., Namba, T., Nakano, M. and Shiraki, K. (1996b). Assay for Antiviral Activity of Herbal Extracts using Their Absorbed Sera. *Chem. Pharm. Bull. (Tokyo)* 44: 1270–1272.

Kurokawa, M., Tsurita, M., Brown, J., Fukuda, Y. and Shiraki, K. (2002). Effect of Interleukin-12 Level Augmented by Kakkon-to, A Herbal Medicine, on the Early Stage of Influenza Infection in Mice. *Antiviral Res.* 56: 183–188.

Kurokawa, M., Watanabe, W., Shimizu, T., Sawamura, R. and Shiraki, K. (2010). Modulation of Cytokine Production by 7-Hydroxycoumarin in Vitro and its Efficacy against Influenza Infection in Mice. *Antiviral Res.* 85: 373–380.

Li, H., Yin, S., Wang, Y. and Sato, T. (2012). Persistent Fluorescence-Assisted $TiO_{2-x}N_y$-Based Photocatalyst for Gaseous Acetaldehyde Degradation. *Environ. Sci. Technol.* 46: 7741–7745.

Lu, S.Y., Wu, D., Wang, Q.L., Yan, J., Buekens, A.G. and Cen, K.F. (2011). Photocatalytic Decomposition on Nano-TiO_2: Destruction of Chloroaromatic Compounds. *Chemosphere* 82: 1215–1224.

McLean, R.L. (1961). General Discussion: The Mechanism of Spread of Asian Influenza. *Am. Rev. Respir. Dis.* 83: 36–38.

Moser, M.R., Bender, T.R., Margolis, H.S., Noble, G.R., Kendal, A.P. and Ritter, D.G. (1979). An Outbreak of Influenza aboard a Commercial Airliner. *Am. J. Epidemiol.* 110: 1–6.

Murphy, B.R., Chalhub, E.G., Nusinoff, S.R., Kasel, J. and Chanock, R.M. (1973). Temperature-Sensitive Mutants of Influenza Virus. 3. Further Characterization of the ts-1(E) Influenza A Recombinant (H3N2) Virus in Man. *J. Infect. Dis.* 128: 479–487.

Rizzo, L. (2009). Inactivation and Injury of Total Coliform Bacteria after Primary Disinfection of Drinking Water by TiO_2 Photocatalysis. *J. Hazard. Mater.* 165: 48–51.

Schulman, J.L. and Kilbourne, E.D. (1962). Airborne Transmission of Influenza Virus Infection in Mice. *Nature* 195: 1129–1130.

Shiraki, K., Daikoku, T., Yoshida, Y., Takemoto, M., Okuda, T., and Himaki, T. (2011). Aerosol Associated Influenza Virus Infect5ivity and its Inactivation by Photocatalysis. *Clinical Virology* 39: 268–275 (in Japanese).

Takahashi, K., Furuta, Y., Fukuda, Y., Kuno, M., Kamiyama, T., Kozaki, K., Nomura, N., Egawa, H., Minami, S. and Shiraki, K. (2003). In Vitro and in Vivo Activities of T-705 and Oseltamivir against Influenza Virus. *Antiviral Chem. Chemother.* 14: 235–241.

Takahashi, Y. (2011). Structure and Function: An Air Filter Named Virus Eliminater which Uses Ultra Micro-photocatalyst. *Clinical Virology* 39: 263–267 (in Japanese).

Vallejo, M., Fresnedo San Roman, M., Ortiz, I. and Irabien, A. (2014). Overview of the PCDD/Fs Degradation Potential and Formation Risk in the Application of Advanced Oxidation Processes (AOPs) to Wastewater Treatment. *Chemosphere* 118C: 44–56.

Xie, X., Li, Y., Chwang, A.T., Ho, P.L. and Seto, W.H. (2007). How Far Droplets Can Move in Indoor Environments--Revisiting the Wells Evaporation-Falling Curve. *Indoor Air* 17: 211–225.

Xie, X., Li, Y., Sun, H. and Liu, L. (2009). Exhaled Droplets Due to Talking and Coughing. *J. R. Soc. Interface* Suppl 6: S703–714.

Yang, S., Lee, G.W., Chen, C.M., Wu, C.C. and Yu, K.P.

(2007). The Size and Concentration of Droplets Generated by Coughing in Human Subjects. *J. Aerosol Med.* 20: 484–494.

Zan, L., Fa, W., Peng, T. and Gong, Z.K. (2007). Photocatalysis Effect of Nanometer TiO_2 and TiO_2-Coated Ceramic Plate on Hepatitis B Virus. *J. Photochem. Photobiol., B* 86: 165–169.

Received for review, October 23, 2014
Revised, January 22, 2015
Accepted, February 4, 2015